Scaling of Electrokinetic Transport in Nanometer Channels

R. Qiao and N. R. Aluru*

Department of Mechanical and Industrial Engineering, Beckman Institute for Advanced Science and Technology, University of Illinois at Urbana-Champaign, Urbana, Illinois 61801

Received May 3, 2005. In Final Form: July 8, 2005

Electrokinetic transport is a popular transport mechanism used in nanofluidic systems, and understanding its scaling behavior is important for the design and optimization of nanofluidic devices. In this article, we report on the scaling of electroosmotic flow and ionic conductivity in positively charged slit nanochannels by using continuum and atomistic simulations. The effects of confinement and surface charge are discussed in detail. In particular, we found that the viscosity of the interfacial water increases substantially as the surface charge density increases and the electrophoretic mobility of the interfacial ions decreases. We show that such effects can influence the scaling of the electrokinetic transport in confined nanochannels significantly.

1. Introduction

Electrokinetic transport of water and ions in nanometer channels and pores plays a crucial role in many engineering and biological systems (e.g., fuel cells, ion channels, and chemical analysis devices[1−5]). Understanding the scaling of electrokinetic transport as a function of various parameters (e.g., channel size, bath concentration, surface charge density, etc.) is important for establishing design rules and for exploring the design space. Continuum simulations[6−9] can provide useful insights into the electrokinetic transport in micro- and nanofluidic systems, and the scaling of electrokinetic transport using continuum simulations has already been investigated.[5,9−11] However, the accuracy of continuum theories in nanometer channels can be an issue.[12,13] In nanochannels, the critical dimension of the channel can be comparable to the size of the fluid molecule, and a significant amount of the fluid in the channel is in contact with the channel surface. Thus, the molecular nature of the fluid/ion and surface effects, which are neglected in the continuum modeling of electrokinetic transport, can become important factors influencing the fluid/ion transport inside the channel. For example, the transport properties of the ions (e.g., electrophoretic mobility and diffusion coefficient) may no longer be taken as their bulk values in highly confined nanochannels or in channels with a high surface charge density. Since atomistic simulations (e.g., molecular dynamics simulation) involve very few assumptions and the atomistic nature of the fluid and ions is modeled explicitly, they are useful tools to use in studying electrokinetic transport in nanochannels. As atomistic simulations are computationally very expensive compared to continuum simulations, they have not been used widely in the past, and the relatively few studies focused on specialized pores.[14] However, with the continuous improvement in computer performance, atomistic simulation of electrokinetic transport has become increasingly more affordable and has been used by several groups recently.[12−17]

In this article, we report on the scaling of electrokinetic transport in slit nanochannels. Specifically, we investigated the scaling of electroosmotic flow as a function of surface charge density and the scaling of the ionic conductivity of the nanochannel as a function of surface charge density, bath concentration, and channel width. In prior studies, the scaling of electrokinetic transport has been investigated using classical continuum theories,[5,10,11,18] where the molecular nature of the fluid and the ions is neglected. Here, we compare the scaling of electrokinetic transport by using molecular dynamics (MD) and continuum theories. We will limit our discussion to positively charged nanochannels because recent studies indicated that electrokinetic transport can be more sensitive to positive surface charge than to negative surface charge.[19] We show that the water viscosity and the electrophoretic mobility of ions can change substantially as the surface charge density and the channel dimension changes, and this can influence the scaling of both the electroosmotic flow and the ionic conductivity significantly.

* Corresponding author. E-mail: aluru@uiuc.edu. http://www.uiuc.edu/∼aluru.

(1) Eikerling, M.; Kharkats, Y.; Kornyshev, A.; Volfkovich, Y. *J. Electrochem. Soc.* **1998**, *145*, 2684−2692.
(2) Hille, B. *Ion Channels of Excitable Membranes*; Sinauer Associates, Inc.: Sunderland, MA, 2001.
(3) Kemery, P. J.; Steehler, J. K.; Bohn, P. W. *Langmuir* **1998**, *14*, 2884−2889.
(4) Kuo, T. C.; Sloan, L. A.; Sweedler, J. V.; Bohn, P. W. *Langmuir* **2001**, *17*, 6298−6303.
(5) Stein, D.; Kruithof, M.; Dekker, C. *Phys. Rev. Lett.* **2004**, *93*, 035901.
(6) Patankar, N. A.; Hu, H. H. *Anal. Chem.* **1998**, *70*, 1870−1881.
(7) Ermakov, S. V.; Jacobson, S. C.; Ramsey, J. M. *Anal. Chem.* **1998**, *70*, 4494−4504.
(8) Mitchell, M. J.; Qiao, R.; Aluru, N. R. *J. Microelectromech. Syst.* **2000**, *9*, 435−449.
(9) Daiguji, H.; Yang, P. D.; Majumdar, A. *Nano Lett.* **2004**, *4*, 137−142.
(10) Hayes, M. A.; Kheterpal, I.; Ewing, A. G. *Anal. Chem.* **1993**, *65*, 27−31.
(11) Poppe, H.; Cifuentes, A.; Kok, W. T. *Anal. Chem.* **1996**, *68*, 888−893.
(12) Freund, J. *J. Chem. Phys.* **2002**, *116*, 2194−2200.
(13) Qiao, R.; Aluru, N. R. *J. Chem. Phys.* **2003**, *118*, 4692−4701.
(14) Lynden-Bell, R. M.; Rasaiah, J. C. *J. Chem. Phys.* **1996**, *105*, 9266−9275.
(15) Marry, V.; Dufreche, J. F.; Jardat, M.; Turq, P. *Mol. Phys.* **2003**, *101*, 3111.
(16) Thompson, A. P. *J. Chem. Phys.* **2003**, *119*, 7503.
(17) Qiao, R.; Aluru, N. R. *Phys. Rev. Lett.* **2004**, *92*, 198301.
(18) Zhou, J. D.; Cui, S. T.; Cochran, H. D. *Mol. Phys.* **2003**, *101*, 1089−1094.
(19) Qiao, R.; Aluru, N. R. *Colloids Surf., A,* accepted for publication, 2005.

10.1021/la0511900 CCC: $30.25
Published on Web 08/19/2005

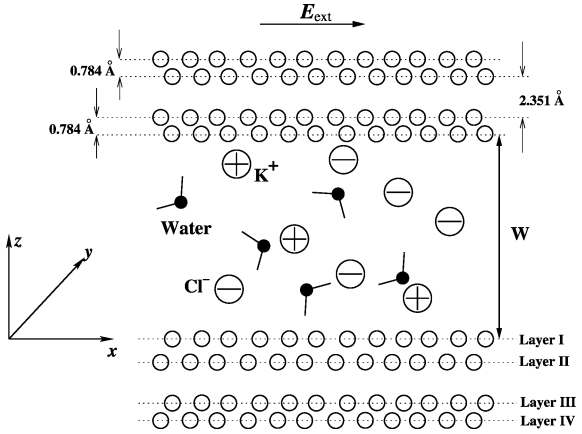

Figure 1. Schematic of the channel system under investigation. The two channel walls are symmetric with respect to the channel center line. For the coordinate system chosen, $z = 0$ corresponds to layer I of the lower channel wall.

The rest of the article is organized as follows. We first present the simulation system and the methods in the next section, and then we present results on the scaling of electroosmotic flow as a function of surface charge. In the following section, we discuss the scaling of ionic conductivity as a function of channel width and surface charge. In particular, we introduce two nondimensional numbers, α_{conf} and β_{sc}, to account for the effect of confinement and surface charge on the ionic conductivity.

2. Simulation Methods

For electrokinetic transport in a straight flat channel with a uniform charge density on the channel walls (Figure 1), the continuum description is based on the Poisson−Boltzmann (PB) equation (1) and the Stokes equation (2)

$$\frac{\partial^2\psi(z)}{\partial z^2} = -\frac{e}{\epsilon_0\epsilon_r}\sum_{i=1}^{N}\tilde{z}_i c_{i,\infty} e^{-\tilde{z}_i e\psi(z)/k_B T} \tag{1}$$

$$\frac{\mathrm{d}}{\mathrm{d}z}\left(\eta(z)\frac{\mathrm{d}u_{eo}(z)}{\mathrm{d}z}\right) + \sum_{i=1}^{N} e\tilde{z}_i c_i(z) E_{ext} = 0 \tag{2}$$

where $\psi(z)$ is the electrical potential at position z, e is the electron charge (i.e., 1.6×10^{-19} C), ϵ_0 is the permittivity of vacuum, ϵ_r is the relative permittivity of the fluid (taken as 81[20]), N is the number of ionic species in the channel (here $N = 2$), $\tilde{z}_i$ is the valency of ionic species i, $c_{i,\infty}$ is the concentration of ion i in the bath connected to the channel, k_B is the Boltzmann constant, T is the temperature, $\eta(z)$ is the water viscosity at position z (taken as 0.743 mPa·s[13]), u_{eo} is the electroosmotic velocity, and E_{ext} is the external electrical field applied along the channel length direction (x direction).

The boundary conditions for eqs 1 and 2 are

$$\frac{\mathrm{d}\psi(z)}{\mathrm{d}z}\Big|_{z=\delta_1, W-\delta_1} = \mp\frac{\sigma_s}{\epsilon_0\epsilon_r} \tag{3}$$

$$u(z)|_{z=\delta_2, W-\delta_2} = 0 \tag{4}$$

where σ_s is the surface charge density of the channel wall, W is the channel width, and δ_1 and δ_2 are the closest approach of the ion and water to the channel wall, respectively.[15] We note that δ_1 and δ_2 are typically not known and need to be obtained from molecular theory or simulations. For the system we investigated here, δ_1 and δ_2 are found to be approximately 0.33 and 0.16 nm, respectively.

The ionic flux J_i has two components in the present system, namely, an electrical migration component

$$J_i^{mig} = \int_{\delta_1}^{W-\delta_1} \tilde{z}_i \mu_i^e(z)\, c_i(z) E_{ext}\, \mathrm{d}z \tag{5}$$

and a convection component

$$J_i^{eo} = \int_{\delta_1}^{W-\delta_1} u_{eo}(z)\, c_i(z)\, \mathrm{d}z \tag{6}$$

where $\mu_i^e(z)$ is the electrophoretic mobility of ion i at position z. The conductivity of the channel is given by

$$\kappa = \frac{1}{(W - 2\delta_1)E_{ext}}\sum_{i=1}^{N}\tilde{z}_i F J_i \tag{7}$$

where F is the Faraday constant and $J_i = J_i^{mig} + J_i^{eo}$.

Figure 1 shows the schematic diagram of the channel system used in the MD simulations. The system consists of a slab of KCl solution sandwiched between two walls. Each wall is made up of four layers of silicon atoms oriented in the ⟨111⟩ direction. The silicon atoms in the innermost layer of the channel wall (layer I of the lower channel wall and its counterpart in the upper channel wall, see Figure 1) were assigned small partial charges to produce the desired surface charge density, σ_s. The water is modeled by using the SPC/E model, and the ions are modeled as charged Lennard-Jones (LJ) atoms. The LJ parameters for the O−O and Si−O pairs were taken from the Gromacs force field,[21] and the LJ parameters for the ion−ion and ion−O pairs were taken from ref 22.

MD simulations were performed with a modified Gromacs 3.0.5.[21] Periodic boundary conditions are used in the x and y directions. The temperature of the fluid was maintained at 300 K by coupling the fluid atoms to a Nose thermostat.[23] To avoid biasing the velocity profile, only the velocity component in the direction orthogonal to the flow was thermostated.[24] The electrostatic interactions are computed by using the PME algorithm with a slab correction,[25] and all other interactions are computed by using a cutoff scheme with a cutoff radius of 1.1 nm. Other simulation details can be found in ref 13. Starting from a random configuration, the system was simulated for 1.0 ns to reach steady state. After that, a production run of 5−15 ns was performed. To study the scaling behavior of the electrokinetic transport, we performed simulations with different surface charge densities and bath concentrations. Note that in the present MD simulations, where the channel system is not explicitly connected to an external bath, the corresponding bath concentration (c_∞) of the channel system needs to be computed indirectly. To compute c_∞, we note that, in a channel wide enough such that the ion distribution in the central portion of the channel can be described accurately by the Poisson−Boltzmann equation, the concentrations of K^+ and Cl^- ions at the channel center ($c_{K^+,cent}$ and $c_{Cl^-,cent}$) can be

(20) van der Spoel, D.; van Maaren, P.; Berendsen, H. *J. Chem. Phys.* **1998**, *108*, 10220−10230.
(21) Lindahl, E.; Hess, B.; van der Spoel, D. *J. Mol. Model.* **2001**, *7*, 306−317.
(22) Koneshan, S.; Rasaiah, J. C.; Lynden-Bell, R. M.; Lee, S. H. *J. Phys. Chem. B* **1998**, *102*, 4193−4204.
(23) Nose, S. *Mol. Phys.* **1984**, *52*, 255−268.
(24) Barrat, J. L.; Bocquet, L. *Phys. Rev. Lett.* **1999**, *82*, 4671−4674.
(25) Yeh, I.; Berkowitz, M. *J. Chem. Phys.* **1999**, *111*, 3155−3162.

Table 1. Summary of the Simulations Performed

case no.	W (nm)	σ_S (C/m^2)	no. water molecules	no. K^+ ions	no. Cl^- ions
1	2.40	0	1367	2	2
2	2.40	0	1361	5	5
3	2.40	0	1355	8	8
4	2.40	0	1341	15	15
5	2.40	0	1329	21	21
6	3.49	0	2116	6	6
7	3.49	0	2106	11	11
8	3.49	0	2094	17	17
9	3.49	0	2068	30	30
10	3.49	0	2054	37	37
11	3.49	0.02	2094	16	21
12	3.49	0.04	2090	16	26
13	3.49	0.08	2104	4	24
14	3.49	0.08	2096	8	28
15	3.49	0.08	2082	15	35
16	3.49	0.08	2062	25	45
17	3.49	0.08	2042	35	55
18	3.49	0.13	2086	4	36
19	3.49	0.13	2076	9	41
20	3.49	0.13	2070	15	47
21	3.49	0.13	2050	25	57
22	3.49	0.13	2030	35	67

related to the external bath concentration by $c_\infty = \sqrt{c_{K^+,cent} c_{Cl^-,cent}}$.[26]

The electrokinetic transport was driven by an external electrical field, E_{ext}, applied along the channel in the x direction. Because of the extremely high thermal noise, a strong electrical field ($|E_{ext}| = 0.2$ V/nm) was used in our simulations so that the fluid/ion velocity can be retrieved with reasonable accuracy. The ion distribution and electroosmotic velocity profiles are obtained by using the binning method. The velocity of the ions, $u_i(z)$, is computed by tracking their trajectories, and the electrophoretic mobility of ion i is computed by $\mu_i^e(z) = |u_i(z) - u_{eo}(z)|/E_{ext}$. Table 1 summarizes the various simulations performed in this article.

3. Scaling of Electroosmotic Flow

To quantify electroosmotic flow in a nanochannel, following ref 11, we define an average electroosmotic mobility

$$\bar{\mu}_{eo} = \frac{1}{W - 2\delta_2} \int_{\delta_2}^{W-\delta_2} \frac{u_{eo}(z)}{E_{ext}} dz \qquad (8)$$

Figure 2 shows the scaling of $\bar{\mu}_{eo}$ versus σ_s in a 3.49 nm channel when the bath concentration of the KCl solution is 0.6 M. We observe that (1) continuum theory overestimates $\bar{\mu}_{eo}$ for all σ_s investigated and the deviation is especially significant for high surface charge densities and (2) for the range of σ_s studied, continuum theory predicts an almost linear increase in $\bar{\mu}_{eo}$ as σ_s increases, whereas the MD simulation indicates that at low surface charge densities (e.g., $\sigma_s < 0.04$ C/m^2) $\bar{\mu}_{eo}$ increases with increasing σ_s and at high surface charge densities (e.g., $\sigma_s > 0.08$ C/m^2) $\bar{\mu}_{eo}$ decreases with increasing σ_s.

To understand the deviation, we computed the ion distribution and velocity profile in the channel when the surface charge density is 0.08 C/m^2. Figure 3 shows the counterion (Cl^-) concentration obtained from the PB equation (1) and the MD simulation. The co-ion concentration is not shown because its contribution to the electroosmotic flow is small. We observe that the MD simulation predicts a much higher first concentration peak

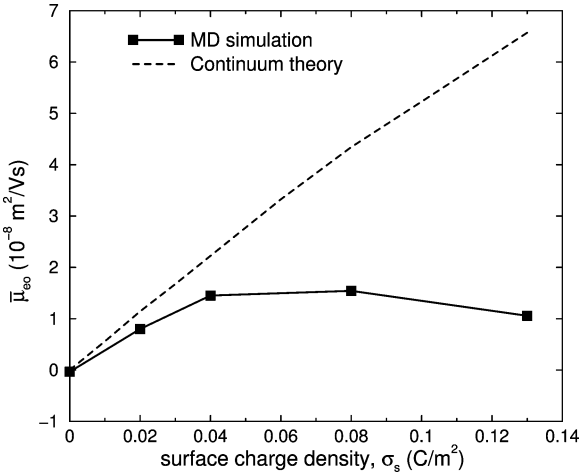

Figure 2. Scaling of the average electroosmotic mobility in a 3.49-nm-wide channel with the surface charge density as obtained from MD and continuum simulations. The bath concentration of the KCl solution is 0.6 M.

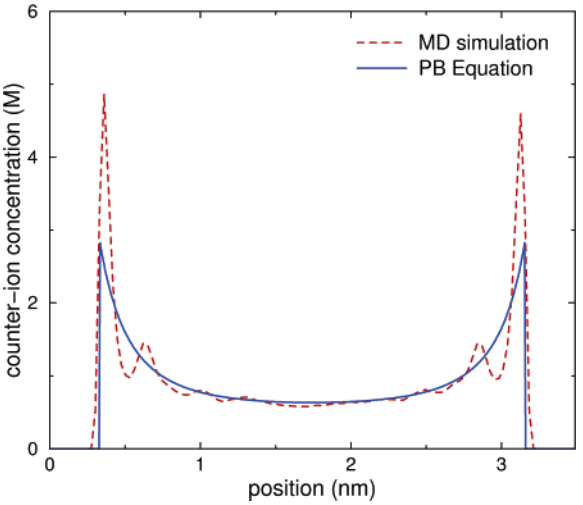

Figure 3. Counterion (Cl^-) concentration profile in a 3.49-nm-wide channel ($\sigma_s = 0.08$ C/m^2, $c_\infty = 0.6$ M) obtained from the PB equation and the MD simulation.

compared to the PB equation and there is an additional second peak at 0.61 nm from the surface. These observations are similar to what were reported earlier,[12,13] and the deviation originates mainly from the molecular nature of the ion and the discreteness of the water molecules, which are not accounted for in the PB equation.

Figure 4a compares the electroosmotic velocity profile in the channel obtained from (i) the Stokes equation with ion concentration from the PB equation as input, (ii) the Stokes equation with MD ion concentration as input, and (iii) MD simulation. A constant viscosity, $\eta = 0.743$ mPa·s, was used in the Stokes equation. We observe that the Stokes equation solution using the ion concentration from the MD simulation is lower compared to the velocity obtained from the Stokes equation using the ion concentration from the PB equation. This indicates that the overestimation of the electroosmotic mobility by the continuum theory is partly caused by the inaccuracy of the PB equation in predicting the ion distribution. However, we note that the velocity obtained from the Stokes equation using the ion concentration from MD as input still overestimates the electroosmotic velocity predicted by the MD simulation. This can be attributed to the higher water viscosity near the channel surface. To

(26) Qiao, R.; Aluru, N. R. *Int. J. Multiscale Comput. Eng.* **2004**, *2*, 173−188.

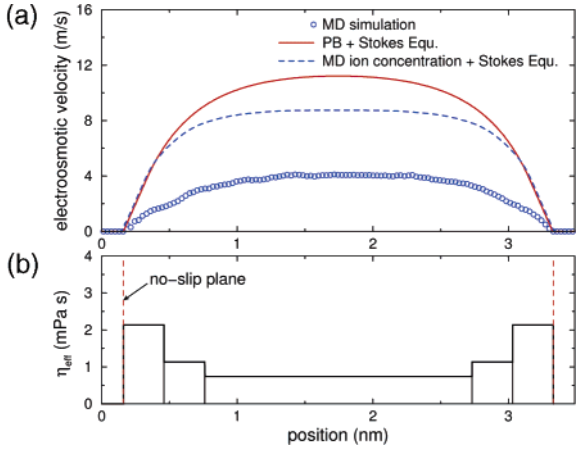

Figure 4. (a) Water velocity profiles in a 3.49-nm-wide channel ($\sigma_s = 0.08$ C/m^2, $c_\infty = 0.6$ M) obtained from the Stokes equation with the ion concentration from the PB equation as input (solid line), the Stokes equation with MD ion concentration as input (dash line), and MD simulation (circles). (b) Effective water viscosity across the channel for the case studied in panel a.

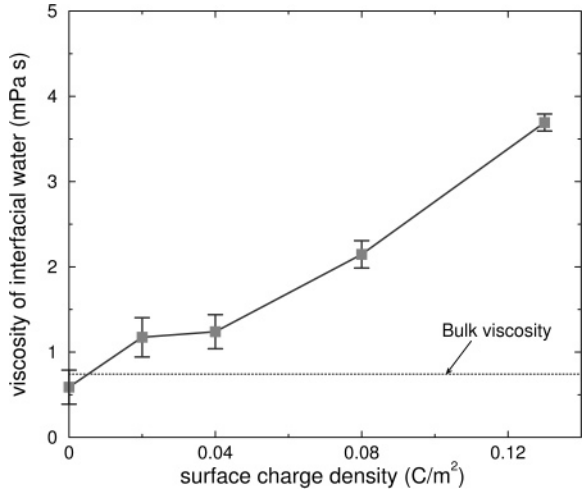

Figure 5. Variation of the effective viscosity of the interfacial water with the surface charge density. Here the interfacial water is taken as the first water layer from the surface.

quantify this, we divide the channel into five bins (0.16−0.46 nm, 0.46−0.76 nm, 0.76−2.73 nm, 2.73−3.03 nm, and 3.03−3.33 nm) and compute the effective viscosity in each bin. (Here we assume that the viscosity in each bin is constant.) Specifically, we substitute the ion concentration from the MD simulation into the Stokes equation (2) and require that the solution of the Stokes equation match the MD velocity at the edge of each bin and at the channel center (z = 1.745 nm). Figure 4b shows the effective viscosity distribution in the channel. We observe that the water viscosity near the channel surface is much higher compared to that of near the channel center. This is consistent with earlier reports.[12,13] Though the exact mechanism is not yet clear, it is usually attributed to the strong electrical field and high ion and water concentrations near the charged surface.[27]

We further investigated how the effective viscosity of the interfacial water (here taken as the first layer of water from the surface) varies with the surface charge density. Figure 5 shows that as σ_s becomes more positive the viscosity of the interfacial water increases dramatically

(27) Hunter, R. *Zeta Potential in Colloid Science: Principles and Applications*; Academic Press: London, 1981.

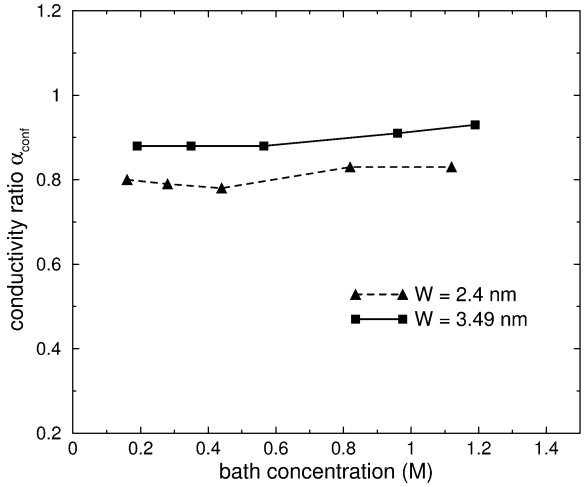

Figure 6. Scaling of the conductivity ratio, α_{conf}, with bath concentration and channel width as predicted by the MD simulations. α_{conf} is a measure of the effect of confinement on the channel conductivity.

and attains a value much larger than the bulk viscosity. Because the viscosity variation is not accounted for in the continuum theory, it overestimates the electroosmotic velocity, particularly at high surface charge densities, as stated in observation 1. Another consequence of the viscosity increase in the interfacial layer with the surface charge density is that, as stated in observation 2, though the net driving force for the electroosmotic flow increases as the surface charge density increases, the electroosmotic velocity will increase much more slowly compared to the continuum prediction and could even decrease because of the higher viscosity near the channel wall.

4. Scaling of Ionic Conductivity

In this section, we investigate the scaling of ionic conductivity in nanochannels as a function of the channel width, bath concentration, and surface charge density using both continuum and molecular dynamics simulations.

To account for the effect of confinement on the ionic conductivity of a nanochannel, we introduce a nondimensional number, α_{conf}, which is defined as

$$\alpha_{conf} = \frac{\kappa_0}{\kappa_\infty} \tag{9}$$

where κ_0 is the conductivity of a nanochannel with zero surface charge density connected to an external bath of concentration c_∞ and κ_∞ is the conductivity of the bulk electrolyte at a concentration of c_∞. Because the continuum theory neglects confinement effects, it can be easily shown that α_{conf} is equal to 1.0. Figure 6 shows the variation of α_{conf} with bath concentration in two nanochannels with widths of 3.49 and 2.4 nm. We observe that, over the range of c_∞ and channel widths investigated here, α_{conf} shows a weak dependence on the bath concentration. We also observe that for a larger channel width (e.g., 3.49 nm) the effect of confinement on the ionic conductivity is small and as the channel width decreases (e.g., 2.4 nm) the confinement effect becomes more important. This is consistent with what was reported in ref 18, where the axial diffusion coefficient of a Cl^- ion in a nanopore of 3.0 nm diameter is found to be close to its bulk value, and its value decreases as the pore size becomes smaller.

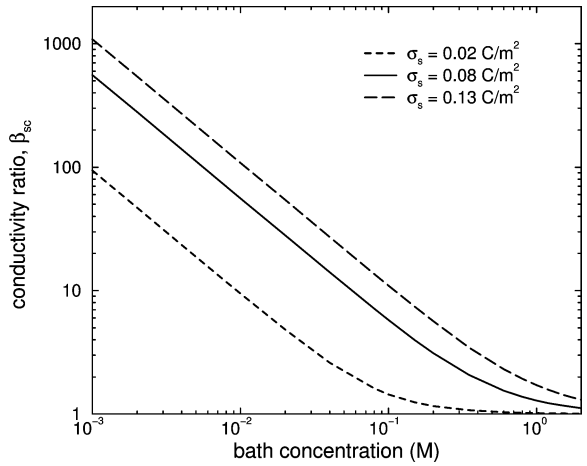

Figure 7. Scaling of the conductivity ratio, β_{sc}, obtained from continuum calculations for a 3.49-nm-wide channel with the surface charge and the bath concentration. The mobilities of K^+ and Cl^- ions are taken as 7.62×10^{-8} and 7.91×10^{-8} m^2/V·s, respectively.[29] β_{sc} is a measure of the change in conductivity of the channel in the presence of a surface charge.

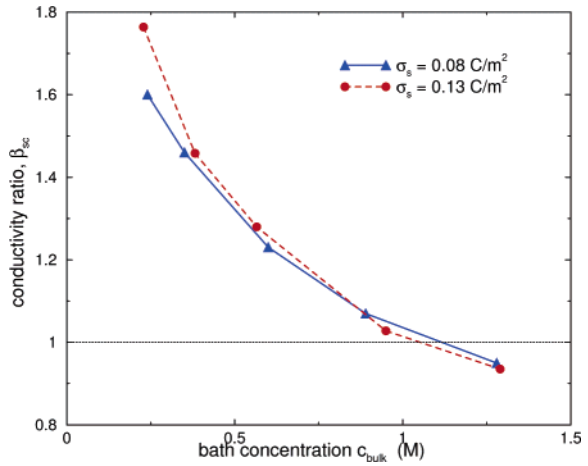

Figure 8. Scaling of the conductivity ratio, β_{sc}, obtained from the MD simulation for a 3.49-nm-wide channel with the surface charge and the bath concentration.

Typically, solid surfaces immersed in an electrolyte solution carry a nonzero charge.[28] Though such a surface charge may not cause a noticeable change in the conductivity of microchannels, it can change the conductivity of nanochannels substantially. For example, it was recently shown that for a bulk concentration of less than 0.1 mM the conductivity of a 70-nm-wide slit channel can be entirely dominated by the surface charge.[5] To account for the effect of the surface charge on the ionic conductivity of a nanochannel, we introduce another nondimensional number, β_{sc}, which is defined as

$$\beta_{sc} = \frac{\kappa_{sc}}{\kappa_0} \tag{10}$$

where κ_{sc} is the conductivity of the nanochannel when the surface charge is not zero and κ_0 is the conductivity of the same channel when the surface charge density is zero. We will first examine how β_{sc} scales with the continuum theory. The mathematical model, similar to that described in ref 5, is given by eqs 1−6. Figure 7 shows the scaling of β_{sc} for a 3.49-nm -wide channel as a function of surface charge and bath concentration. We observe that β_{sc} increases with decreasing bath concentration and increasing surface charge density. At low bath concentrations ($c_\infty < 10^{-2}$ M) and high surface charge densities ($\sigma_s > 0.08$ C/m^2) β_{sc} is on the order of 100 or higher, indicating that the conductivity is entirely dominated by the surface charge. This is mainly caused by the fact that, at high σ_s and low c_∞, the average ion concentration inside the channel is much larger compared to that of the bath electrolyte because of the attraction of counterions to the charged channel surface (concentration enrichment). As the bath concentration increases, though the average ion concentration inside the channel is high when compared to the ion concentration inside the channel when the surface charge is zero, the conductivity ratio becomes smaller. As a result, β_{sc} decays toward its asymptotic value of 1.0.

In the above calculations, the electrophoretic mobility of the ions inside the nanochannel is assumed to be the bulk value regardless of the surface charge density and the channel width. Because the electrophoretic mobility of the ions can be influenced by the channel width and the surface charge, we have also used MD simulations to study the conductivity ratio, β_{sc}. Figure 8 shows the scaling of β_{sc} for a 3.49-nm-wide channel with the surface charge and the bath concentration. Comparing Figure 8 with Figure 7, we observe that, though the scaling of β_{sc} follows a similar trend, there are two important differences.

First, MD simulations indicate that β_{sc} can be less than 1.0 at high bath concentrations ($c_\infty > 1.1$ M) whereas β_{sc} is never less than 1.0 in the continuum simulations. This is mainly caused by the fact that, at high positive surface charge densities, the electrophoretic mobility of the counterions in the nanochannel can be much smaller compared to its value when the nanochannel has zero surface charge density. In such a scenario, the decrease in the electrophoretic mobility of the counterions due to the presence of surface charge can be more important than the surface-charge-induced ion concentration enrichment in the channel. Because the concentration enhancement is less significant for high c_∞, $\beta_{sc} < 1.0$ occurs mainly at high c_∞. To understand this quantitatively, we compute the conductivity ratio, β_{sc}, when $c_\infty = 1.25$ M and $\sigma_s = 0.13$ C/m^2. The average Cl^- ion (counterion) concentration inside the channel, obtained from MD simulations, is 2.00 M (i.e., 60% higher than its bath concentration). Figure 9 shows the electrophoretic mobility and concentration distribution of the Cl^- ion across the channel obtained from the MD simulation. We observe that near the positively charged channel wall the electrophoretic mobility of the Cl^- ion is only about 20% of its value at the channel center. Because a significant number of the Cl^- ions are accumulated near the positively charged surface, the average electrophoretic mobility of the Cl^- ion in the channel is much lower than its value when the nanochannel has zero surface charge density, leading to a smaller conductivity compared to κ_0.

Second, MD simulation indicated that, at high bath concentrations ($c_\infty > 0.5$ M), β_{sc} increases slightly or even decreases with increasing surface charge density. This can be seen more clearly in Figure 10a, where the variation of β_{sc} as a function of the surface charge density is shown. (The bath concentration is kept at 0.6 M.) We observe that at low σ_s ($\sigma_s < 0.08$ C/m^2) MD simulations predict a much slower increase of β_{sc} compared to continuum theory and at high σ_s ($\sigma_s > 0.08$ C/m^2) β_{sc} almost saturates. To

(28) Lyklema, J. *Fundamentals of Interface and Colloid Science*; Academic Press: San Diego, CA, 1995.
(29) Atkins, P. W. *Physical Chemistry*; Oxford University Press: Oxford, U.K., 1990.

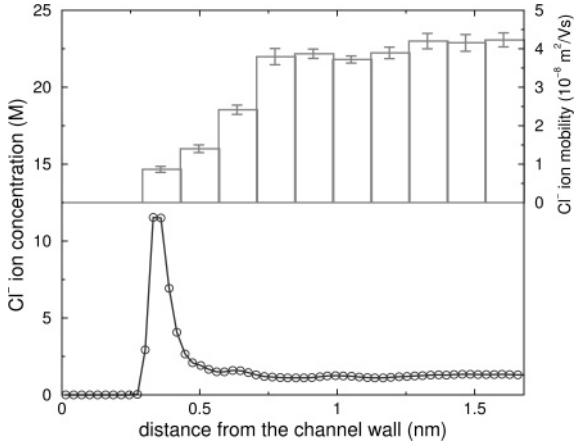

Figure 9. Variation of the Cl^- ion concentration (left y axis) and electrophoretic mobility (right y axis) in a 3.49-nm-wide channel ($\sigma_s = 0.13$ C/m^2, $c_\infty = 1.25$ M).

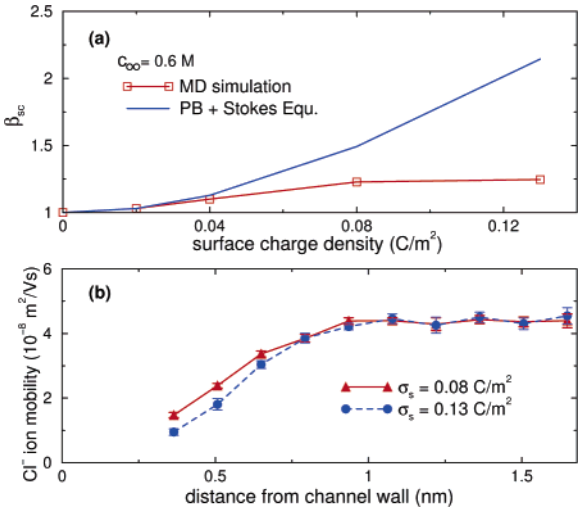

Figure 10. (a) Comparison the conductivity ratio, β_{sc}, obtained from continuum and MD simulations for a 3.49-nm-wide channel. The bath concentration is 0.6 M. (b) Variation of the electrophoretic mobility of a Cl^- ion in a 3.49 nm channel for a surface charge densities of 0.08 and 0.13 C/m^2. The bath concentration is 0.6 M.

understand such scaling behavior, we study the variation of the electrophoretic mobility of the counterion as σ_s increases.

Figure 10b shows the electrophoretic mobility of the Cl^- ion across the channel when σ_s is 0.08 and 0.13 C/m^2, respectively. We observe that as σ_s increases the electrophoretic mobility of Cl^- ions near the charged surface decreases. This is consistent with the increase of the interfacial water viscosity discussed in the previous section (i.e., the ion mobility is known to scale inversely with the viscosity of water in which it is immersed[22]). The decrease in electrophoretic mobility tends to reduce the migration component of the ionic current (eq 5), and the increase in interfacial water viscosity tends to reduce the convection component of the ionic current (eq 6 and Figure 2). The combination of these two factors then leads to the scaling behavior shown in Figure 10a.

5. Conclusions

In this article, we reported on the scaling of electrokinetic transport in nanometer slit channels using continuum and MD simulations. MD simulations indicate that as the surface charge density increases the average electroosmotic mobility in a slit nanochannel increases much more slowly compared to that predicted by continuum theory. In addition, although continuum theory predicts that the average electroosmotic mobility increases with surface charge density, MD simulations indicate that for a large surface charge density the average electroosmotic mobility can decrease. The scaling of the average electroosmotic mobility can be explained by the increase in the interfacial water viscosity with the surface charge density. We introduced two dimensionless numbers, namely, the conductivity ratio, α_{conf}, and the conductivity ratio, β_{sc}. α_{conf} is a measure of the change in conductivity of the channel because of confinement, and β_{sc} is a measure of the change in conductivity of the channel because of the surface charge. MD simulations indicate that α_{conf} is slightly less than 1 for a 3.49-nm-wide channel but decreases as the channel width decreases. Continuum simulations indicate that for a low bath concentration and for a small channel width (e.g., 3.49 nm) β_{sc} can be several orders of magnitude larger than 1 and the ionic conductivity is dominated by the surface charge. For a high bath concentration and for a moderate-to-high surface charge (e.g., $\sigma_s > 0.08$ C/m^2), continuum calculations predict that β_{sc} approaches 1.0, whereas MD simulations predict that β_{sc} becomes less than 1.0. The scaling of β_{sc} to less than 1.0 can be explained by the decrease of the electrophoretic mobility of the interfacial ions near the channel wall and by the increase of the interfacial water viscosity when the surface charge density increases.

Acknowledgment. This research was supported by the NSF Science and Technology Center of Advanced Materials for the Purification of Water with Systems (CAMPWS, cooperative agreement CTS-0120978) and a grant from NSF (0140496).

LA0511900